Journal of Alloys and Compounds 504S (2010) S222–S225

Contents lists available at ScienceDirect

Journal of Alloys and Compounds

journal homepage: www.elsevier.com/locate/jallcom

Primary crystallization reactions in Al-based metallic glass alloys

J.H. Perepezko*, S.D. Imhoff

University of Wisconsin-Madison, Department of Materials Science and Engineering, 1509 University Avenue, Madison, WI 53706, USA

ARTICLE INFO

Article history:
Received 4 July 2009
Received in revised form 18 January 2010
Accepted 10 February 2010
Available online 18 February 2010

Keywords:
Nanostructures
Amorphization
Precipitation

ABSTRACT

For Al-based metallic glasses primary crystallization is effective in yielding nanoscale microstructures with crystal densities upto 10^{22} m^{-3} or higher. The crystallization kinetics determinations support a heterogeneous nucleation from quenched in atom arrangements that act as catalysts, but the kinetics are also influenced by transient effects. The decaying growth rate at long times can be related to diffusion field impingement, but other factors operate at short times. The primary crystallization reaction can be controlled effectively by suitable minor solute substitution to enhance nanocrystal densities upto 10^{23} m^{-3} at refined sizes or to inhibit nucleation to lower densities of about 10^{20} m^{-3}. These developments offer new opportunities for control of nanoscale microstructures and also challenges for the understanding of the reaction mechanisms.

1. Introduction

Through an understanding of thermodynamic quantities such as enthalpies of mixing as well as refinements to topological instability criteria, contemporary bulk metallic glasses have been designed to exhibit remarkable stability against crystallization [1–3]. Interestingly, aluminum based alloy glasses have lagged in the drive for the lower critical cooling rates necessary for bulk metallic glass synthesis. However, they have presented new and intriguing properties of glasses that motivate a deeper examination of how local atomic arrangements determine the properties. The identification of ordering beyond the first nearest neighbor coordination combined with changes in crystallization behavior due to different amorphization pathways indicates the importance of these arrangements [4,5]. Moreover, they support the concept of an energy landscape [6] that describes the relative energetic stability of a particular state as a framework for analyzing amorphous phases. At the same time the observation of extraordinarily high nucleation product densities approaching 10^{24} nanocrystals m^{-3} [7] has been puzzling; however, new evidence indicates that heterogeneous and transient nucleation effects are critical in interpreting the nanoparticle development [8]. In the present limited discussion some of the highlights of primary crystallization behavior in amorphous Al alloys are reviewed along with new observations to identify directions for further examination.

1.1. Primary crystallization kinetics

The kinetics of primary crystallization of amorphous alloys have been examined by a variety of techniques. For example, isothermal differential scanning calorimetry (DSC) traces of Al–Ni–Ce [9] and Al–Sm amorphous alloys [10,11] have illustrated distinct monotonically decreasing rates of heat release with time, indicating a growth controlled process and suggesting that the transformation results from the growth of pre-existent atom arrangements. These results, however, are in contrast with other DSC experiments on Al–Ni–Ce [9], Al–Fe–Gd [12], Al–Y–Fe [13], and Al–(Gd–X)–Ni [14] alloys that show exothermic peaks only after an observed incubation time, which is a clear indication of a nucleation and growth mechanism. Upon closer examination of the crystallization microstructures it is evident that the apparent dichotomy in DSC results is a reflection of the strong composition and product structure dependence of the initial crystallization reaction. Clearly, microstructural information is essential for complete interpretation of kinetics measurements.

In another approach, several nanocrystal size distribution analysis studies have been used to characterize the crystallization of some Al amorphous alloys. In a number of alloys [15–17] there is the early development of a high nanocrystal particle density that increases modestly as the reaction continues with distinctly sluggish growth. In other investigations [15,17–19] size distributions of α-Al particles in Al–Y–Fe, Al–Ni–Nd, and Al–Ni–Y alloy systems were found to be consistent with a transient heterogeneous nucleation mechanism. As a result, a large density (10^{21} to 10^{23} m^{-3} or greater) of undetermined heterogeneous sites was proposed to exist in the amorphous precursor. Clearly, a full analysis of nanocrystallization requires the concurrent application of both approaches. Moreover, the amorphous precursor state is of critical importance to the stability of quenched Al-based glasses.

* Corresponding author. Tel.: +1 608 263 1678.
E-mail address: perepezk@engr.wisc.edu (J.H. Perepezko).

0925-8388/$ – see front matter © 2010 Elsevier B.V. All rights reserved.
doi:10.1016/j.jallcom.2010.02.063

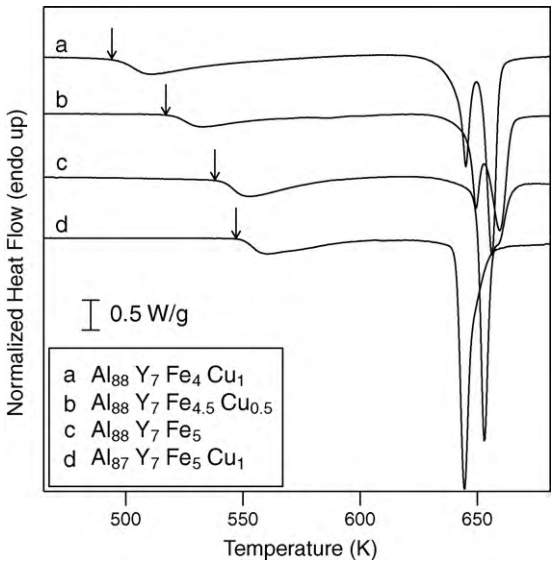

Fig. 1. Continuous heating DSC (20 K/min) traces of several Al–Y–Fe–Cu compositions showing the strong dependence of primary crystallization on Cu substitution.

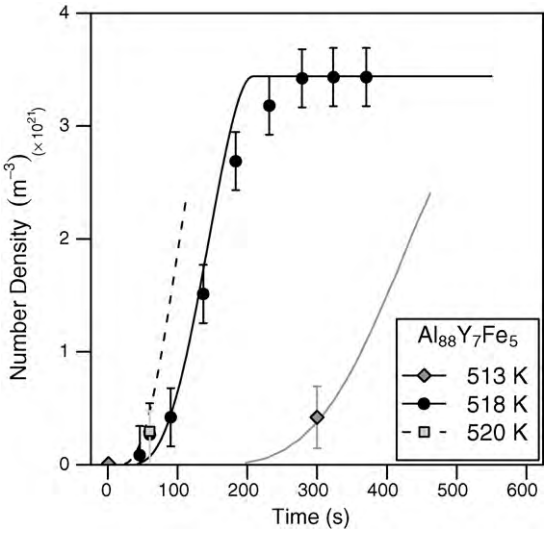

Fig. 2. Measured and calculated (solid curves) Al nanocrystal number density for $Al_{88}Y_7Fe_5$ as a function of time at three temperatures that defines the transient period.

As a result of the initial studies of primary crystallization kinetics several proposals involving solute-based clusters [20], coupled fluxes [21] or phase separation [22] have been advanced to account for the high nanocrystal density, However, recent insight from fluctuation electron microscopy indicating that Al-like structural arrangements represent MRO in amorphous Al alloys has provided new evidence for the role of the structural heterogeneities that can act to influence nanocrystal nucleation and modify transient kinetics behavior [8]. From these developments it is evident that a standard steady state nucleation kinetics analysis is not appropriate to interpret the nanostructure development. When the atomic arrangements in amorphous phases are spatially heterogeneous, at least on the size scales relevant to nucleation, it is necessary to include the catalytic influence of the heterogeneities and examine transient effects in order to develop a realistic kinetics model [8].

1.2. Crystallization control through solute substitution

Changes in the temperature range and the shape of the primary crystallization peak as well as the nanoparticle density after annealing are related to the alteration of crystallization behavior, as shown in Fig. 1. Moreover, small additions of Cu (substituting for Fe in $Al_{88}Y_7Fe_5$) have been shown to decrease the average size of the Al nanocrystals by enhancing nucleation at temperatures where the growth rate is sluggish. Although Cu substitutions in amorphous Fe alloys can refine the nanocrystal size, the Cu clustering behavior exhibited in Fe-based amorphous alloys [23–26] is not reproduced in Al glasses [27]. Thus, the Cu solute substitution affects nucleation in a different precursor mode that is observed, as a increase in volume fraction of the MRO within the amorphous matrix with substitution of Cu for Fe [28].

At the same time, substitution of Cu for Al results in an increase in the crystallization onset temperature, T_x. Similar behavior has been reported in Al–Ni–Sm amorphous alloys [29] where Cu substitution for Ni decreases T_x while substitution for Al increases T_x. Other reports of transition metal substitution for Al also reveal an increase in T_x [30]. The dual role of minor solute substitution to either increase or decrease T_x depending on the substituted component is intriguing. It seems unlikely that a minor solute addition level would yield a significant change in the thermodynamic driving free energy for crystallization. Moreover, if the minor solute level influenced the crystal/glass interface energy, it is difficult to understand how the effect of the same amount of solute substitution would depend on the nature of the substituted component. Instead, it seems more probable that the solute substitution influences the MRO characteristics and the transport behavior.

1.3. Transient kinetics behavior

A primary crystallization kinetics model based upon catalysis by MRO regions [28] can account for the direction of change in the onset of crystallization on heating due to the changes in MRO number density with composition. For a 1 at% substitution of Cu for Fe in $Al_{88}Y_7Fe_5$ a change in the crystallization temperature, ΔT_x of ~50 K is observed (Fig. 1). In order to account for the magnitude of ΔT_x it is necessary to consider transient nucleation behavior as well. It should be noted that in much of the literature surrounding the ternary Al–Y–Fe system, the idea of pure growth of quenched in features as opposed to nucleation is prevalent. While the evidence from isothermal DSC traces is consistent with a pure growth mechanism, TEM investigation has shown that this result is misleading. Treatment at temperatures close to T_x precludes observation of transient effects that affect the amorphous phase precursor and subsequent crystallization characteristics. A representation of some of the results is shown in Fig. 2, where a clear transient is not only present, but also changes by an order of magnitude over an interval of 7 K. If the trend in transient behavior shown in Fig. 2 were the same for $Al_{88}Y_7Fe_4$ Cu_1 where the crystallization temperature drops precipitously, then steady state nucleation would not be expected at such low temperatures. Indeed, one telling feature of the substitutions is shown in Fig. 3 where an $Al_{88}Y_7Fe_5$ sample annealed for 1 h at 518 K has a nanocrystal density of 3.0×10^{21} m^{-3} and an $Al_{87}Y_7Fe_5Cu_1$ sample annealed under the same conditions has a nanocrystal density of only 6.9×10^{20} m^{-3} indicating a significant decrease in the overall observed nucleation rate. Further, in an $Al_{88}Y_7Fe_4Cu_1$ sample, crystallization would occur well before an annealing temperature of 518 K could be reached, but after annealing at 443 K, a much larger number density than either of the two other samples, of 1.1×10^{22} m^{-3} is measured.

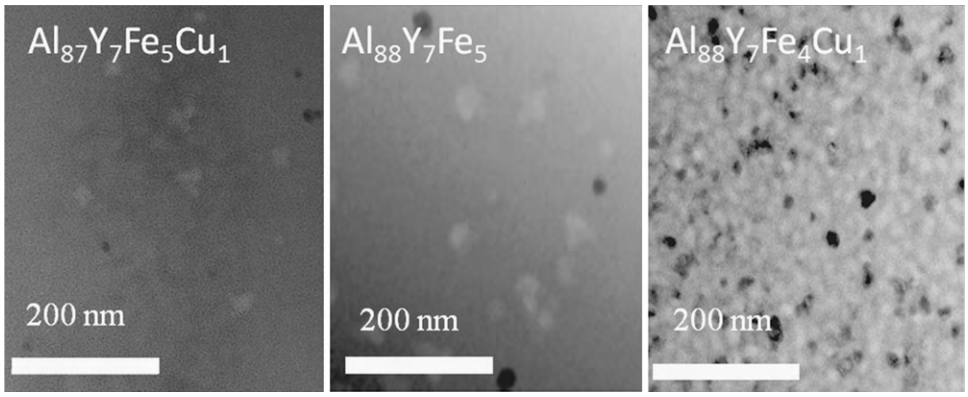

Fig. 3. TEM micrographs showing the particle population of (a) $Al_{87}Y_7Fe_5Cu_1$ annealed at 518 K, (b) $Al_{88}Y_7Fe_5$ annealed at 518 K and (c) $Al_{88}Y_7Fe_4Cu_1$ annealed at 443 K all for 1 h.

1.4. Structural relaxation

For some amorphous alloys such as $Al_{84}Y_6Ni_4Co_2Sc_4$ T_g has been measured [31], however; for $Al_{88}Y_7Fe_5$ and similar amorphous alloys, a T_g is not observed clearly during continuous heating, but the potential reasons for this have not been identified. For instance, if the heat capacity change, ΔC_p, that underlies the glass transition is small, the signal may be concealed by concurrent exothermic signals such as incipient crystallization or structural relaxation. To explore this, relaxation experiments have been carried out at temperatures and times which do not result in observable crystals. For an amorphous $Al_{88}Y_7Fe_5$ alloy annealed at 508 K for increasing times an endothermic T_g signal begins to separate from the baseline and grows in intensity with annealing Fig. 4. Similarly, $Al_{88}Y_7Fe_{4.5}Cu_{0.5}$ annealed at 478 K for varying times also gives an endothermic signal during reheating, Fig. 5. If the substitution is made for aluminum, a T_g signal can be observed without prior relaxation treatment at either the Cu 0.5 at% [30] or 1 at% level. In order to confirm these results, the reversibility of the apparent T_g signal has been established by cycling the relaxed sample about T_g.

The presence of a clear T_g signal in both of these alloys and the fact that the temperature change of the endotherm tracks with the crystallization signal reveals that the dynamics within the matrix are changing dramatically with minor solute substitution levels. The link between a composition dependent volume fraction and MRO number density and the atomic mobility clearly warrants further investigation.

2. Summary

Amorphous Al alloys present a number of intriguing challenges to the contemporary understanding of amorphous phase formation, stability and crystallization. While the widely accepted guidelines for amorphous phase formation seem to apply to component selection, the typical Al-rich compositions and relatively high crystallization temperatures suggest another role for the specific solutes in facilitating stability. At the same time, the strong composition dependence of the thermal stability, glass transition behavior, and the remarkably high nucleation density developed during primary crystallization are unusual. Moreover, structural determinations reveal a heterogeneous structure that is characterized by a high level of Al-like MRO. When these characteristic features are considered together it is evident that the conventional kinetics analysis should be modified to take account of the heterogeneous behavior of the matrix and the changes in local transport as a function of composition. The measured MRO size distributions and number densities can account for the high nucleation rates by lowering the activation barrier for nucleation and including tran-

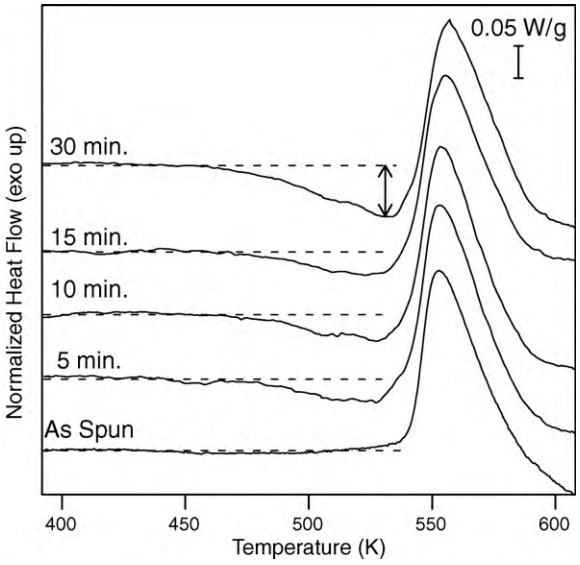

Fig. 4. Constant heating (20 K/min) DSC traces of $Al_{88}Y_7Fe_5$ after several annealing treatments at 508 K.

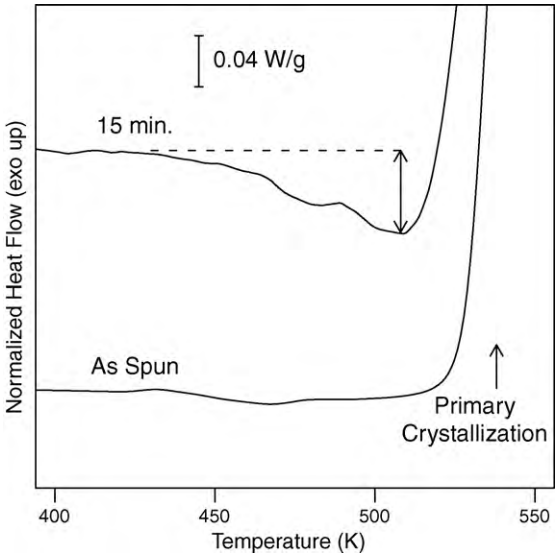

Fig. 5. Constant heating (60 K/min) DSC traces of $Al_{88}Y_7Fe_{4.5}Cu_{0.5}$ after annealing at 478 K.

sient behavior. The identification of a glass transition within the ternary $Al_{88}Y_7Fe_5$ samples as well as the change in T_g as a function of solute substitution suggests that the MRO regions can act to drastically change the transport behavior. The strong influence of specific minor solute substitutions on the nanocrystal number density is an open issue, but the effectiveness of the solute substitution suggests a possible route to bulk glass formation and offers a useful tool for achieving reproducible nanocomposite microstructures.

Acknowledgments

We are pleased to thank Professor P.M. Voyles and F. Yi for valuable discussion and collaboration.

References

[1] T. Zhang, A. Inoue, T. Masumoto, J. Non-Cryst. Solids 156–158 (1993) 473.
[2] A. Inoue, Prog. Mater. Sci. 43 (1998) 365.
[3] A. Inoue, Bulk Amorphous Alloys: Practical Characteristics and Applications, Trans Tech Publications Ltd., Switzerland, 1999.
[4] A. Sadoc, O. Heckmann, V. Nassif, O. Proux, J.-L. Hazemann, L.Q. Xing, K.F. Kelton, J. Non-Cryst. Solids 353 (2007) 2758.
[5] W.G. Stratton, J. Hamann, J.H. Perepezko, P.M. Voyles, X. Mao, S.V. Khare, Appl. Phys. Lett. 86 (2005) 141910.
[6] F.H. Stillinger, Science 267 (1995) 1935.
[7] D.V. Louzguine-Luzgin, A. Inoue, J. Mater. Res. 21 (2006) 1347.
[8] J.H. Perepezko, S.D. Imhoff, R.J. Hebert, J. Alloys Compd. (2009), doi:10.1016/j.jallcom.2009.10.051.
[9] M.K. Miller, A. Cerezo, M.G. Hetherington, G.D.W. Smith, Atom Probe Field Ion Microscopy, Oxford University Press, Oxford, 1996.
[10] J.H. Perepezko, R.J. Hebert, W.S. Tong, J. Hamann, H.R. Rosner, G. Wilde, Mater. Trans. JIM 44 (2003) 1982.
[11] G. Wilde, R.I. Wu, J.H. Perepezko, Riso International Symposiom of Materials Science, vol. 22, 2001, p. 429.
[12] H. Chen, Y. He, G.J. Shiflet, S.J. Poon, Nature 367 (1994) 541.
[13] Z.C. Zhong, X.Y. Jiang, A.L. Greer, Philos. Mag. B 76 (1997) 505.
[14] A.K. Gangopadhyay, K.F. Kelton, Philos. Mag. A 80 (2000) 1193.
[15] P. Rizzi, M. Baricco, L. Battezzati, P. Schumacher, A.L. Greer, Mater. Sci. Forum 235–238 (1997) 409.
[16] D.R. Allen, J.C. Foley, J.H. Perepezko, Acta Mater. 46 (1998) 431.
[17] A. Revesz, L.K. Varga, S. Surinach, M.D. Baro, J. Mater. Res. 17 (2002) 2140.
[18] M. Calin, U. Koster, Mater. Sci. Forum 269–272 (1998) 749.
[19] M. Calin, A. Rudiger, U. Koster, Mater. Sci. Forum 243–246 (2000) 359.
[20] D.B. Miracle, Acta Mater. 54 (2006) 4317.
[21] K.F. Kelton, Acta Mater. 48 (2000) 1967.
[22] A.K. Gangopadhyay, T.K. Croat, K.F. Kelton, Acta Mater. 48 (2000) 4035.
[23] K. Hono, D.H. Ping, M. Ohnuma, H. Onodera, Acta Mater. 47 (1999) 997.
[24] K. Suzuki, A. Makino, A. Inoue, T. Masumoto, J. Appl. Phys. 70 (1991) 6232.
[25] Y. Yoshizawa, S. Oguma, K. Yamauchi, J. Appl. Phys. 64 (1988) 6044.
[26] K. Suzuki, N. Kataoka, A. Inoue, A. Makino, T. Masumoto, Mater. Trans. JIM 31 (1990) 743.
[27] K. Hono, Y. Zhang, A. Inoue, T. Sakurai, Mater. Trans. JIM 36 (1995) 909.
[28] W.G. Stratton, P.M. Voyles, Ultramicroscopy 108 (2008) 727.
[29] Y. Zhang, P.J. Warren, A. Cerezo, Mater. Sci. Eng. A327 (2002) 109.
[30] K.S. Bondi, A.K. Gangopadhyay, Z. Marine, T.H. Kim, A. Mukhopadhyay, A.I. Goldman, W.E. Bhuro, K.F. Kelton, J. Non-Cryst. Solids 353 (2007) 4723.
[31] D.V. Louzguine-Luzgin, A. Inoue, W.J. Botta, Appl. Phys. Lett. 88 (2006) 011911.